Nuclear Instruments and Methods in Physics Research B 402 (2017) 388–392

Contents lists available at ScienceDirect

Nuclear Instruments and Methods in Physics Research B

journal homepage: www.elsevier.com/locate/nimb

First measurements of betatron radiation at FLAME laser facility

A. Curcio [a,b,*], M. Anania [a], F. Bisesto [a,b], E. Chiadroni [a], A. Cianchi [a], M. Ferrario [a], F. Filippi [a,b], D. Giulietti [c], A. Marocchino [a], F. Mira [b], M. Petrarca [d], V. Shpakov [a], A. Zigler [a,e]

[a] INFN-LNF, via Enrico Fermi 40, 00044 Frascati (Rome), Italy
[b] Department of Physics, "Sapienza" University of Rome, Piazzale A. Moro 2, I-00185 Rome, Italy
[c] Physics Department of the University and INFN, Largo Bruno Pontecorvo 3, 56127 Pisa, Italy
[d] Department of Basic and Applied Sciences for Engineering (SBAI) and INFN-Roma1, "Sapienza" University of Rome, Via A. Scarpa 14, 00161 Rome, Italy
[e] Racah Institute of Physics, Hebrew University, Jerusalem 91904, Israel

ARTICLE INFO

Article history:
Received 6 December 2016
Received in revised form 14 February 2017
Accepted 21 March 2017
Available online 31 March 2017

Keywords:
Blowout regime
Betatron radiation
X-rays

ABSTRACT

The first results on betatron radiation obtained in laser-plasma acceleration experiments at the FLAME laser facility are presented. The diagnostic apparatus for the X-ray detection available at the facility is described together with the experimental setup for the generation of betatron radiation.

1. Introduction

The betatron radiation is the wiggler-like synchrotron radiation [1–14] emitted by electrons accelerated in laser-plasma wakefields [16]. In the strongly non-linear regime, i.e. at laser extremely relativistic intensities, the wakefield accelerating structure for the electrons is bubble-like [17,18] and the electrons are self-injected from the rear of the bubble inside the accelerating and focusing region, completely depleted from electrons by the strong ponderomotive laser potential at its passage through the underdense plasma. Here we present the first results on betatron X-ray detection performed at the FLAME laser facility [19–21] of the National Laboratories of Frascati of INFN. The X-ray diagnostics available at the facility are briefly described and finally it is shown how they have been strategically used for the detection of betatron radiation in self-injection laser-plasma acceleration experiments.

2. X-ray diagnostics at FLAME facility

The hard X-ray spectrometer (Fig. 1) available at the FLAME laser facility is the *CdTe* (model AMPETEK X-123CdTe) [22], having an active area of 9 mm^2, a 1000 μm semiconductor thickness and a 100 μm *Be* window. The detector is mounted on a thermoelectric cooler for reducing the electronic noise. It combines, in a single package, the *CdTe* drift X-ray detector and preamplifier, the digital pulse processor (AMPTEK DP5) and MCA, and the Power Supply (AMPTEK PC5). It works in an energy range of $5 \div 150$ keV with energy resolution less than 1.2 keV FWHM at 122 keV.

The soft X-ray detector at the facility is the Andor DX 434 BR-DD (Fig. 2), where BR-DD stays for Back illuminated CCD, Deep Depletion NIR AR coating. The active pixels are 1024×256, the pixel size is 26×26 μm, the image area is 26.6×6.7 mm^2, it is vacuum compatible down to 10^{-5} millibar and below and the maximum cooling is about $-100°$.

Both the *CdTe* spectrometer and the CCD-X camera utilized as spectrometer can work only with low X-ray fluxes, i.e. in single photon counting. The X-ray scintillator [23] (Fig. 3) foil is based on $Ti-doped\ CsI$ single crystals, the pixel size is ~ 50 μm while the foil area is 10 cm^2.

The X-ray scintillator is positioned before the X-ray spectrometer and the X-ray filters because it can work at high-flux. In this way the scintillator allows the measurement of spatial distribution of the X-ray radiation simultaneously to the spectrum detection, which is performed at low flux after damping the radiation (Fig. 5).

3. Experimental results

A self-injection experimental campaign was performed at the SPARC-LAB test facility (INFN-LNF) by using the laser FLAME. The main pulse characteristics were changed according to various tests

* Corresponding author at: Department of Physics, "Sapienza" University of Rome, Piazzale A. Moro2, I-00185 Rome, Italy.
E-mail address: curcioalexander@gmail.com (A. Curcio).

http://dx.doi.org/10.1016/j.nimb.2017.03.106
0168-583X/

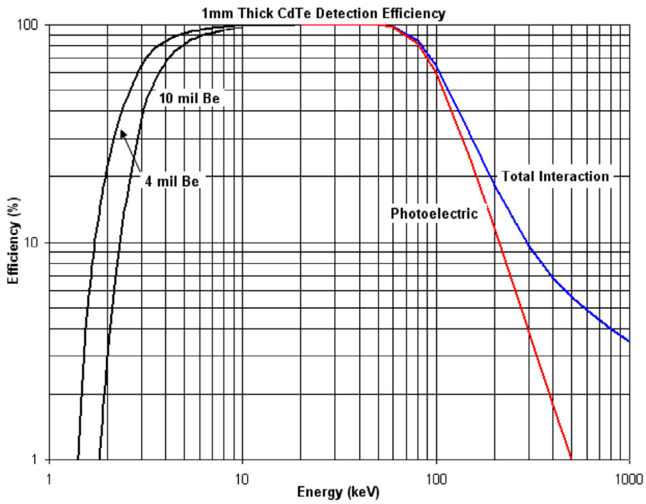

Fig. 1. Detection efficiency of the *CdTe* hard X-ray spectrometer.

and they ranged within the values $\sim 1-1.5$ J energy, delivered in 30–35 fs over a 10 μm diameter focus. The laser was focused on a *He* gas-jet target. The electron density of the generated plasma was measured through a Mach-Zender interferometer to range as $n_e = 5-10\times 10^{18}$ cm^{-3}, according to the height of the main laser beam with respect to the basis of the nozzle and according to the gas pressure sent into the jet. The maximum acceleration length was measured looking at the extension of the plasma in the interferometric images of the laser propagated through the underdense plasma and it was in the range $L_{acc} \sim 1-2$ mm, according to the diameter of the gas-nozzle and of the plasma density used shot by shot. The energy spectrum of the electrons was measured by using of a magnetic dipole coupled to a scintillator LANEX screen. The regime of laser-plasma interaction, as discussed in Ref. [14], was the bubble regime. At our laser intensity the relativistic parameter $a_0 = 8.5\times 10^{-10}\lambda_0[\mu\mathrm{m}]\sqrt{I_0[\mathrm{W/cm^2}]} > 4$ (where I_0 and λ_0 are the laser intensity and wavelength respectively), therefore as described in Ref [18] we were in the condition for the complete depletion of the electrons behind the laser pulse. The depletion region on the wake of the laser pulse is expected of spherical shape, whence the name "bubble regime". Full 3D PIC simulations (Fig. 4) confirmed this regime of interaction. The simulations were performed with the *ALaDyn* code [24–27] for a driver laser pulse and a background electron plasma density with the same characteristics of the experimental ones. The code predicted a

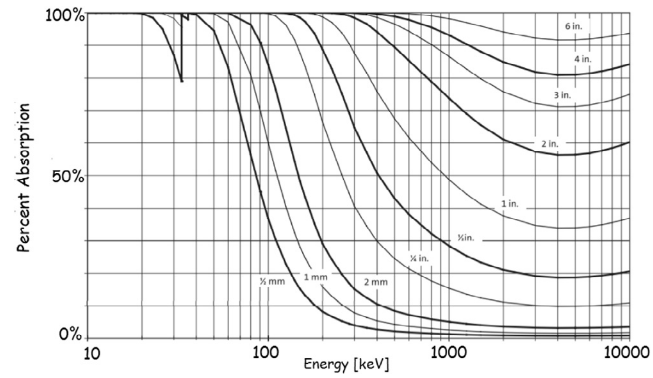

Fig. 3. X-ray scintillator foil based on *Ti − doped CsI* single crystals together with its absorption efficiency for different thicknesses. The foil area is 10 cm^2, the thickness $\sim$ 200 μm.

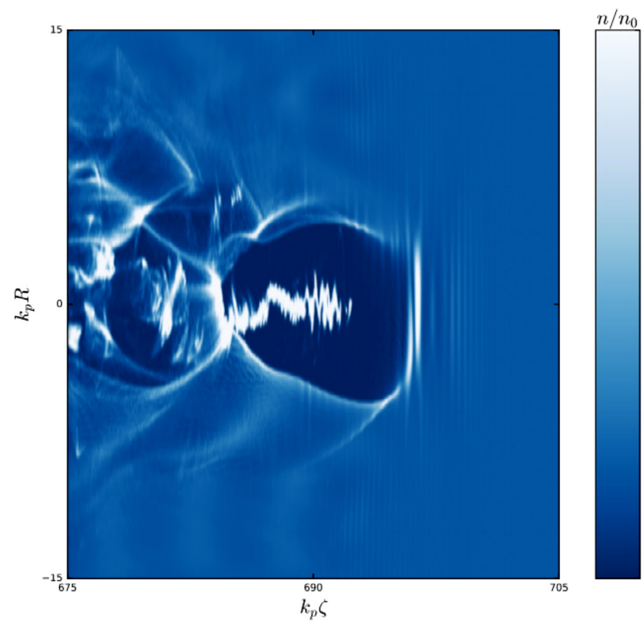

Fig. 4. Example of 2D plasma density plot from PIC Code ALaDyn simulations, in dimensionless units. For the full 3D simulation was used a $1120\times 304\times 304$ moving window, with a longitudinal resolution of 0.05 μm, a transverse resolution of 0.0125 μm and 8 particles per cell. The plasma density is normalized to the unperturbed background density ($n_0 = 1\times 10^{19}$ cm^{-3}). The snapshot is taken at 0.7 mm propagation distance. The laser FWHM duration is 30 fs, while the initial laser diameter is 11.76 μm.

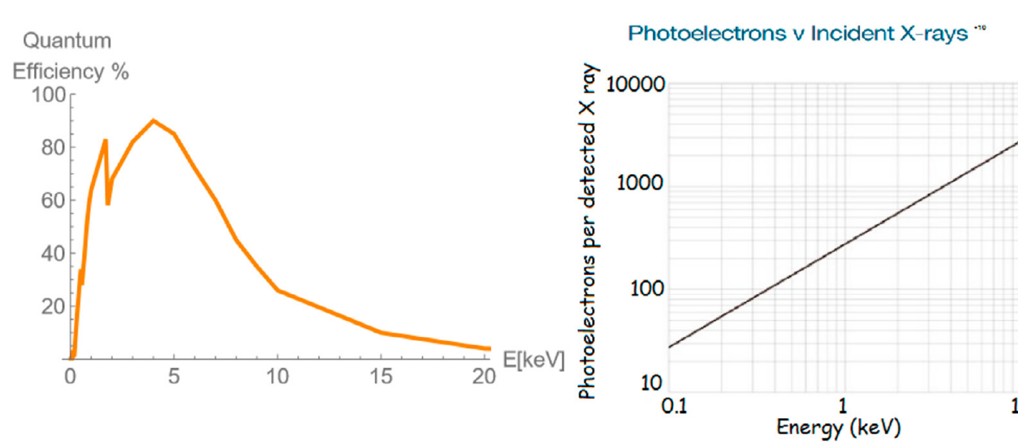

Fig. 2. Andor CCD-X for soft X-ray detection together with its detection efficiency and the number of photoelectrons per detected incident X-ray.